AIP | Applied Physics Letters

High-reflectivity ultraviolet AlGaN/AlGaN distributed Bragg reflectors

O. Mitrofanov, S. Schmult, M. J. Manfra, T. Siegrist, N. G. Weimann et al.

Citation: Appl. Phys. Lett. **88**, 171101 (2006); doi: 10.1063/1.2195547
View online: http://dx.doi.org/10.1063/1.2195547
View Table of Contents: http://apl.aip.org/resource/1/APPLAB/v88/i17
Published by the American Institute of Physics.

High-reflectivity ultraviolet AlGaN/AlGaN distributed Bragg reflectors

O. Mitrofanov,[a] S. Schmult, M. J. Manfra, T. Siegrist, N. G. Weimann, and A. M. Sergent
Bell Laboratories, Lucent Technologies, 600 Mountain Avenue, Murray Hill, New Jersey 07974

R. J. Molnar
MIT Lincoln Laboratory, 244 Wood Street, Lexington, Massachusetts 02420

(Received 15 December 2005; accepted 2 March 2006; published online 24 April 2006)

We demonstrate high-reflectivity crack-free $Al_{0.18}Ga_{0.82}N/Al_{0.8}Ga_{0.2}N$ distributed Bragg reflectors (DBR) for the spectral region around 350 nm grown by molecular-beam epitaxy on thick GaN templates. The structural quality of the DBR layers is maintained by compensating the compressive and tensile stress in each $\lambda/4$ pair. This approach results in the lowest elastic strain energy and allows the growth of thick coherently strained DBRs. A 25 period mirror provides a 26 nm wide stop band centered at 347 nm with the maximum reflectivity higher than 99%. © *2006 American Institute of Physics*. [DOI: 10.1063/1.2195547]

High-quality distributed Bragg reflectors (DBRs) in the ultraviolet region are essential for the development of GaN-based optical devices. In particular, the region around 350 nm is important for devices containing pure GaN as an active medium. The growth of DBRs remains a fundamental challenge in the nitride system. The difficulty lies in maintaining the structural integrity of a relatively thick structure that contains materials with a large lattice constant mismatch and different thermal expansion coefficients. The successful growth of lattice-matched AlGaN/AlInN DBRs with metal-organic vapor phase epitaxy has been reported recently,[1,2] however, it is yet to be demonstrated using molecular-beam epitaxy (MBE). Only a few groups have reported high-reflectivity $Al_xGa_{1-x}N/Al_yGa_{1-y}N$ DBRs.[3–6]

Due to the lattice constant mismatch between GaN and AlN, an $Al_xGa_{1-x}N$ epilayer grown on the GaN substrate experiences in-plane tensile strain. The layer is stable against the introduction of misfit dislocations if its thickness is below the critical thickness defined by the Matthews–Blakeslee criterion.[7] A typical $Al_xGa_{1-x}N/Al_yGa_{1-y}N$ DBR structure is much thicker than the critical layer thickness, and the strain in the structure tends to relax by generating a network of cracks, which degrade the optical quality. However, if the DBR structure is designed to alternate between the tensile and the compressive strain in the layers with different Al content, the in-plane stress in the individual layers counteracts and the epilayers maintain coherency with the substrate throughout the structure.

In this letter, we demonstrate high-reflectivity crack-free $Al_{0.18}Ga_{0.82}N/Al_{0.8}Ga_{0.2}N$ DBRs in which the low Al content layers are under the in-plane compressive stress and the high Al content layers are under the tensile stress. The structures are grown by MBE on GaN templates. We have produced DBR stacks consisting of up to 25 periods that exhibit no cracks. A 25-period DBR provides the maximum reflectivity close to 100% and a 26 nm wide stop band centered at 347 nm.

To compensate for the stress in the individual layers of the DBR structure, and to minimize the elastic strain energy, the lateral lattice constant of the structure must match the average lattice constant $a_0=(a_1d_1+a_2d_2)/(d_1+d_2)$, where $a_{1,2}$ and $d_{1,2}$ are the bulk lattice constant and the thickness of the individual layers, respectively. For a stack of $Al_xGa_{1-x}N/Al_yGa_{1-y}N$ layers, a_0 corresponds to the bulk lattice constant of $Al_XGa_{1-X}N$ with the average Al content $X=(xd_1+yd_2)/(d_1+d_2)$. The average lattice constant a_0 can be set by growing a relaxed $Al_XGa_{1-X}N$ interlayer prior the growth of the DBR stack.

The Al content x and y of the DBR layers are chosen so that the thickness of each layer, determined by the center wavelength of the DBR $d_{1,2}=\lambda_0/4n_{1,2}$, does not exceed the corresponding critical thickness. The DBR structure therefore remains coherently strained with the strain alternating from the compressive in the low Al content layers to the tensile in the high Al content layers. The corresponding stress is compensated for in each pair of the $\lambda/4$ layers such that a DBR structure can be grown without cracks.

The critical misfit defines the thermodynamic boundary between epilayers with a given thickness stable against and susceptible to the dislocation formation. For a mirror with the stop band centered at around 350 nm, the thickness of individual DBR layers is $d=\lambda_0/4n\sim 30-40$ nm. The critical misfit for thickness $d=30$ nm is ~ 0.003 and it corresponds to the variation of the Al content in the DBR layers $X-x\cong y-X\sim 0.15$.[8] However, films with thickness exceeding the critical by a factor of 2 typically remain coherent with the substrate.[9]

The Al content x is chosen high enough to avoid the interband absorption within the stop band. Taking into consideration these constraints, the following DBR structure was grown: The $Al_XGa_{1-X}N$ interlayer with Al content $X=0.5\pm 0.05$ is grown on an initial MBE GaN buffer layer; it is followed by an $Al_xGa_{1-x}N/Al_yGa_{1-y}N$ pair of quarter-wave layers with $x=0.18\pm 0.02$ and $y=0.8\pm 0.1$ repeated $(m-1)$ times; the structure is capped by a $\lambda/4$ layer of $Al_xGa_{1-x}N$. The misfit between the GaN substrate and the interlayer with Al content $X=0.5$ is ~ 0.013. The corresponding critical thickness $d_c<10$ nm $\ll \lambda_0/4n$. Therefore, the interlayer thickness was adjusted to match one-quarter of the central wavelength and to serve as a part of the DBR structure with m $\lambda/4$ pairs.

100 μm thick GaN templates are prepared by hydride vapor phase epitaxy on 2 in. sapphire substrates. The DBR structures are grown on the GaN templates by plasma-

[a]Electronic mail: olegm@lucent.com

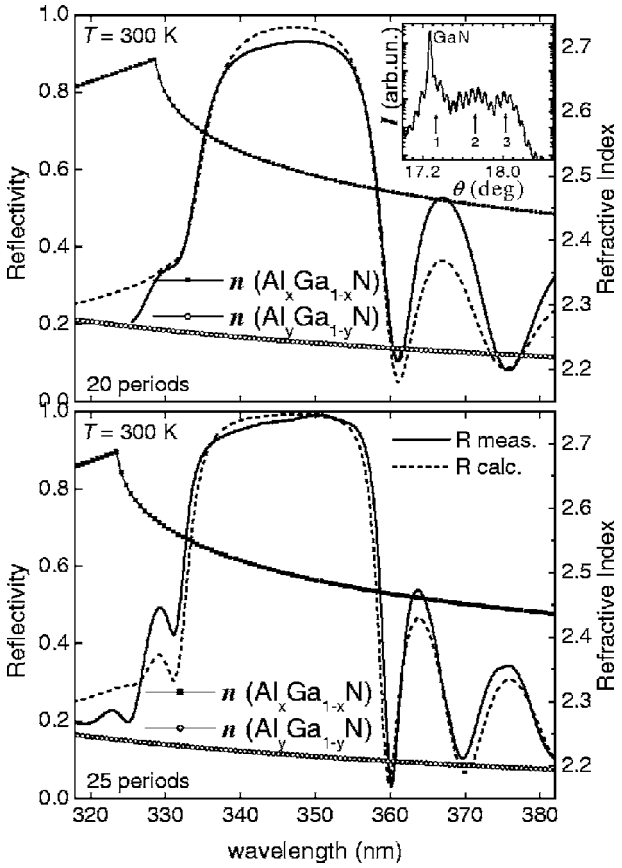

FIG. 1. Reflectivity spectra of $Al_{0.18}Ga_{0.82}N/Al_{0.8}Ga_{0.2}N$ DBRs containing 20 (S1) and 25 (S2) periods of $\lambda/4$ pairs measured at room temperature (solid line), and the refractive index functions (line+symbol) used in the reflectivity calculations (dashed line). The inset shows the x-ray diffraction scan around the (0002) reflex of GaN. The arrows indicate locations of the diffraction peaks that correspond to the DBR layers (1,3) and the interlayer (2).

assisted MBE at 750 °C and the background pressure of 2×10^{-6} Torr under slightly metal-rich conditions at a growth rate of 300 nm/h set by a radio-frequency power of 400 W and nitrogen flow rate of 0.75 sccm. Two Al cells were used for the growth of the alternating AlGaN layers. The cell designated for the high Al content layers is also used for the growth of the interlayer. The growth conditions were proven to produce sharp interfaces, as confirmed by the x-ray analysis of reference superlattice samples. The homogeneity of the layer thickness throughout the structure is confirmed by cross-sectional scanning electron microscopy.

DBR samples are grown with the periods of $d_1+d_2=53$, 67, 74, and 83 nm as determined by high-resolution x-ray diffractometry in ω-2θ geometry. All samples with the period up to 74 nm exhibit no crack formation. The x-ray diffraction scans show compressive strain in the low Al content layers and tensile strain in the high Al content layers (inset of Fig. 1). A 83 nm period sample developed a network of cracks with an average spacing of 5–7 μm clearly visible in the optical microscope. Detailed structural characterization of the samples will be presented elsewhere.[10]

Optical reflectivity spectra of the samples are measured at room temperature and at $T=10$ K using a xenon arc lamp. The room-temperature characteristics of the 74 nm period mirrors are shown in Fig. 1. The 20-pair (S1) and 25-pair (S2) structures produce well-defined stop bands with the maximum reflectivity of 93±1.5% and 99±1.5% and the full

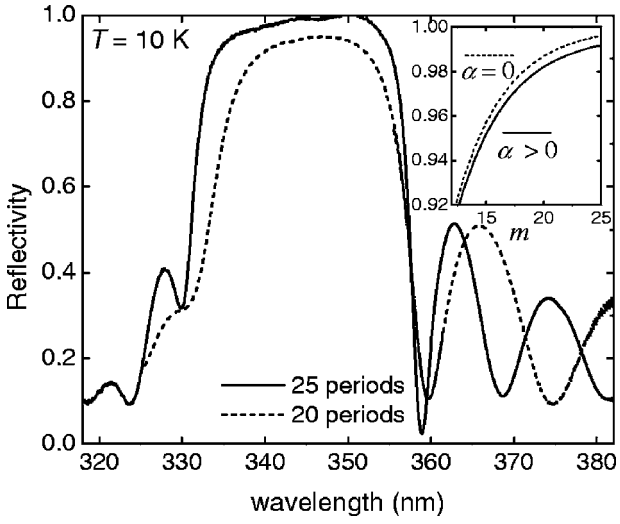

FIG. 2. Reflectivity spectra of $Al_{0.18}Ga_{0.82}N/Al_{0.8}Ga_{0.2}N$ DBRs containing 20 (S1) and 25 (S2) periods of $\lambda/4$ pairs measured at $T=10$ K. Maximum reflectivity of the DBR as a function of the number of $\lambda/4$ pairs m calculated with and without the Urbach band gap absorption tail.

width at half maximum of 25 nm and 26 nm, respectively. The maximum reflectivity is verified by the direct measurement of the reflection coefficient using the frequency-doubled emission from a mode-locked Ti-Sapphire laser tuned to 700 nm. The low-temperature spectra are shown in Fig. 2. The maximum reflectivity increases to 95% for the 20 period sample and to 100% (within the experimental error of ±1.5%) for the 25 period sample.

The reflectivity spectra are used to extract the refractive indices and absorption coefficients of the AlGaN layers. To model the wavelength dependence of the refractive indices, we assume a general model of the real part of the dielectric function in the vicinity of the band gap[11]

$$\epsilon(\lambda) = C + A\frac{\lambda^2}{\lambda_g^2}\left[2 - \left(1+\frac{\lambda_g}{\lambda}\right)^{1/2} - \left(1-\frac{\lambda_g}{\lambda}\right)^{1/2}\right], \qquad (1)$$

where $\lambda_g = hc/E_g$ is the band-gap absorption edge, and A and C are constants that depend on the Al content. The absorption coefficient is assumed to decay exponentially below the band gap according to the Urbach model: $\alpha(E)=\alpha_0 \exp(E-E_g/E_{Ur})$. By varying the parameters of Eq. (1), reflectivity spectra are calculated using the transfer matrix approach and matched to the experimental data (Fig. 1).

The parameters of Eq. (1) used in the calculations are summarized in Table I. Strongly damped oscillations of the reflectivity on the short-wavelength side of the stop band indicate that the absorption edge of the low Al content layer is located immediately next to the stop band. It allows the determination of the absorption edge λ_g for $Al_xGa_{1-x}N$ layers

TABLE I. Parameters of Eq. (1) used to model refractive indices of AlGaN layers in samples S1 and S2.

Sample/layer	E_g (eV)	A	C
S1/$Al_xGa_{1-x}N$	3.77	5.35	4.07
S2/$Al_xGa_{1-x}N$	3.83	5.44	4.04
S1/$Al_yGa_{1-y}N$	4.62	5.98	3.11
S2/$Al_yGa_{1-y}N$	4.70	6.00	3.01

with high accuracy. The absorption coefficient for $Al_xGa_{1-x}N$ layers above the band gap is assumed to be equal to $\alpha_0 = 0.63 \times 10^5$ cm^{-1} (Ref. [12]) and the Urbach parameter $E_{Ur} = 0.045$ eV is adjusted to fit the experimental data.

The calculated reflectivity spectra show a good fit to the experimental data. The corresponding refractive indices modeled by Eq. (1) are shown in Fig. 1. Compared to the values reported in the literature the optical constants determined from the fit appear slightly smaller.[12,13] The index decrease in the low Al content layers is partly attributed to the strain-induced changes in the band-gap structure. The compressive strain results in a positive shift of the absorption edge $\Delta E_g \sim 50$ meV:

$$\Delta E_g = \frac{dE_g}{d\sigma}\Delta\sigma = \frac{E}{1-\nu}\frac{dE_g}{d\sigma}\frac{\Delta a}{a}, \tag{2}$$

where the strain induced coefficient $dE_g/d\sigma = 25\text{meV}/\text{GPa}$,[14] the bulk modulus $E = 200$ GPa, Poisson's ratio $\nu = 0.22$, and the misfit between the $Al_{0.18}Ga_{0.82}N$ and the $Al_{0.5}Ga_{0.5}N$ layer $f = \frac{\Delta a}{a} = 0.008$. The refractive index varies most rapidly in the vicinity of the band gap, and the shift in the band-gap position of the low Al content layers by 50 meV ($\sim$5 nm @ 350 nm) can produce the refractive index decrease of $\Delta n = 0.03$. In addition, a variation of several percent in the composition of AlGaN layers would alter the optical constants.

Factors limiting reflectivity include the refractive index contrast between the $\lambda/4$ layers and intrinsic absorption in the low Al content layer below the band gap. The maximum reflectivity for a DBR consisting of layers with the refractive indices of sample S2 is shown in the inset of Fig. 2. The maximum reflectivity is calculated as a function of the number of periods m assuming no absorption below the band gap. The effect of intrinsic absorption can be seen in the shape of the stop band sloped on the short-wavelength side. The maximum reflectivity for a mirror with the intrinsic absorption below the band gap described by the Urbach model decreases by $\sim$0.5%.

In conclusion, we demonstrate high-reflectivity 25 period $Al_{0.18}Ga_{0.82}N/Al_{0.8}Ga_{0.2}N$ DBRs centered at 347 nm grown by MBE on thick GaN templates. The structural quality of the DBR layers is maintained by balancing the compressive and tensile strains in each $\lambda/4$ pair. This approach results in the lowest elastic strain energy and allows the growth of thick coherently strained DBRs. Reflectivity spectra show a 26 nm wide stop band centered at 347 nm with the maximum reflectivity higher than 99%. The stop band covers the spectral region corresponding to the exciton energies in bulk GaN and AlGaN/GaN quantum wells, and the DBRs can be used to build microcavities with GaN quantum wells as an active medium.

One of the authors (S. S.) would like to thank Hock Min Ng for helpful discussions. The Lincoln Laboratory portion of this work was sponsored by the United States Air Force under Air Force Contract No. FA8721-05-C-0002. The opinions, interpretations, conclusions and recommendations are those of the authors and are not necessarily endorsed by the United States Government.

[1] J.-F. Carlin and M. Ilegems, Appl. Phys. Lett. **83**, 668 (2003).
[2] E. Feltin, J.-F. Carlin, J. Dorzar, G. Christmann, R. Butte, M. Laugt, M. Ilegems, and N. Grandjean, Appl. Phys. Lett. **88**, 051108 (2006).
[3] R. Langer, A. Barski, J. Simon, N. T. Pelekanos, O. Konovalov, R. Andre, and L. S. Dang, Appl. Phys. Lett. **74**, 3610 (1999).
[4] H. M. Ng, T. D. Moustakas, and S. N. G. Chu, Appl. Phys. Lett. **76**, 2818 (2000).
[5] F. Natali, D. Byrne, A. Dussaigne, N. Grandjean, J. Massies, and B. Damilano, Appl. Phys. Lett. **82**, 499 (2003).
[6] T. Wang, R. J. Lynch, P. J. Parbrook, R. Butte, A. Alyamani, D. Sanvitto, D. M. Whittaker, and M. S. Skolnick, Appl. Phys. Lett. **85**, 43 (2004).
[7] J. W. Matthhews and A. E. Blakeslee, J. Cryst. Growth **27**, 118 (1974).
[8] A. D. Bykhovski, B. L. Gelmont, and M. S. Shur, J. Appl. Phys. **81**, 6332 (1997).
[9] O. Ambacher, B. Foutz, J. Smart, J. R. Shealy, N. G. Weimann, K. Chu, M. Murphy, A. J. Sierakowski, W. J. Schaff, L. F. Eastman, R. Dimitrov, A. Mitchell, and M. Stutzmann, J. Appl. Phys. **87**, 344 (2000).
[10] S. Schmult, T. Siegrist, O. Mitrofanov, M. J. Manfra, A. M. Sergent, and R. J. Molnar (unpublished).
[11] P. Y. Yu and M. Cardona, *Fundamentals of Semiconductors* (Springer, New York, 2001).
[12] D. Brunner, H. Angerer, E. Bustarret, F. Freudenberg, R. Hopler, R. Dmitrov, O. Ambacher, and M. Stutzmann, J. Appl. Phys. **82**, 5090 (1997).
[13] N. Antoine-Vincent, F. Natali, M. Michailovic, A. Vasson, J. Leymarie, P. Disseix, D. Byrne, F. Semond, and J. Massies, J. Appl. Phys. **93**, 5222 (2003).
[14] W. Rieger, T. Metzger, H. Angerer, R. Dmitrov, O. Ambacher, and M. Stutzmann, Appl. Phys. Lett. **68**, 970 (1996).